https://doi.org/10.1093/plphys/kiac142 PLANT PHYSIOLOGY 2022: 189: 1220–1225

Plant Physiology®

Letter to the Editor

Loss of SALT OVERLY SENSITIVE 1 prevents virescence in chloroplast K^+/H^+ EFFLUX ANTIPORTER-deficient mutants

Rachael Ann DeTar [1,2], Ricarda Höhner [1], Nikolay Manavski [2], Marius Blackholm [2], Jörg Meurer [2] and Hans-Henning Kunz [1,2,*,†]

1 Plant Physiology, School of Biological Sciences, Washington State University, PO Box 644236, Pullman, Washington 99164-4236, USA
2 LMU Munich, Plant Sciences, Großhaderner Str. 2-4, 82152 Planegg-Martinsried, Germany

*Author for correspondence: kunz@lmu.de
†Senior author

H.-H.K. designed the research. R.A.D. performed most of the experiments with further support from R.H. M.B., N.M., and J.M. carried out RNA blot experiments. R.A.D. and H.-H.K. wrote the paper with edits from N.M. and J.M. H.-H.K. is responsible for contact and ensuring communication.
The author responsible for distribution of materials integral to the findings presented in this article in accordance with the policy described in the Instructions for Authors (https://academic.oup.com/plphys/pages/General-Instructions) is: Hans-Henning Kunz (kunz@lmu.de).

Dear Editor,

The importance of plastid K^+/H^+ EFFLUX ANTIPORTERs (KEAs) for organelle function and photosynthesis has drawn a lot of research interest over the last years (Aranda-Sicilia et al., 2012; Armbruster et al., 2014; Kunz et al., 2014; Wang et al., 2017). Our group recently reported that the loss of KEA1 and KEA2, the two inner envelope membrane carriers, affects ion homeostasis, rRNA processing in the stroma, and concomitant plastid gene expression (PGE). As a consequence, the GENOMES UNCOUPLED 1 (GUN1)-dependent retrograde signaling (RS) pathway is activated to halt organelle biogenesis through suppression of GOLDEN2-LIKE (GLK) transcription factors and their targets, photosynthesis-associated nuclear-encoded genes (PhANGs) (DeTar et al., 2021). These insights were enabled by a unique salt rescue phenomenon inherent to the virescent (pale young leaves) of *kea1kea2* loss-of-function mutants (Kunz et al., 2014). When mutant plants are treated with moderate concentrations of NaCl, they exhibit a recovery in plastid rRNA metabolism, higher rates of PGE, more wild-type (WT)-like expression of nuclear-encoded genes, and finally greener rosettes with higher chlorophyll (Chl) content and increased photosynthetic rates (DeTar et al., 2021). Here, we endeavor to better understand the mechanism of the salt rescue in *kea1kea2* through the isolation and characterization of a genetic suppressor of the *kea1kea2* phenotype.

Plants rely on high cellular K content ($\geqslant$100 mM). Soil salinity or NaCl treatment induce K deprivation in species unadapted to saline habitats (Shin and Adams, 2014). We and others have found that loss of KEA1/2 results in a dangerous K excess in leaf tissue (Höhner et al., 2016; Sánchez-McSweeney et al., 2021). Exogenous NaCl treatment can counter these effects, resetting K^+ concentrations in *kea1-kea2* leaves to WT level (DeTar et al., 2021). This may occur either through reduced K^+ root-level uptake or by preventing K^+ long-distance transfer into leaves. These questions inspired us to test if a similar rescue effect in *kea1kea2* can be achieved without external Na through genetic manipulation of the plant's K:Na ratio via the plasma membrane Na^+/H^+ antiporter (SODIUM OVERLY SENSITIVE) SOS1 (Shi et al., 2000, 2002). SOS1 is thought to extrude Na^+ ions from the root during salt stress and to control long-distance transport of Na^+ via entry or reuptake from the xylem (Shi et al., 2002; Shin and Adams, 2014). *sos1* loss-of-function mutants exhibit decreased K content, lower rates of K^+ uptake, less K^+ root-to-shoot translocation, increased Na level,

Received January 06, 2022. Accepted March 02, 2022. Advance access publication March 23, 2022

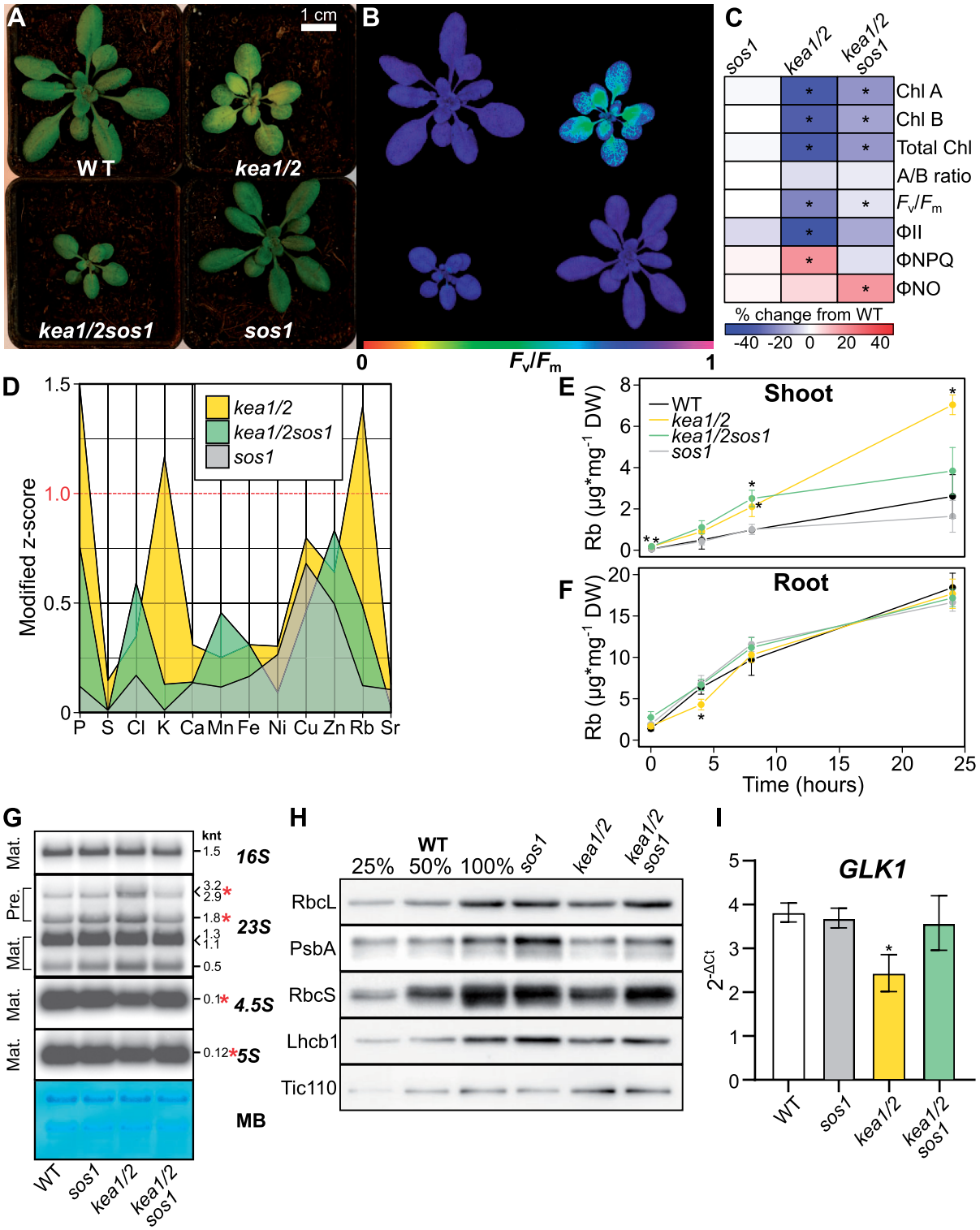

Figure 1 Loss of *SOS1* in the *kea1kea2* background results in phenotypic recovery. A, RGB and B, false color image of the maximum quantum efficiency of PSII (F_v/F_m) for WT, *kea1-1kea2-1*, *sos1-15*, and loss-of-function triple line *kea1-1kea2-1sos1-15*. C, Heatmap showing percent change from WT for assorted parameters. Asterisks denote genotypes where the mean for the given parameter was significantly different from the WT ($P < 0.05$ based on Tukey's HSD test if data for all genotypes were normally distributed, or pairwise Wilcoxon rank sum test if one or more genotype did not exhibit normal distribution of values). Chl parameters include concentration per unit fresh weight for Chl *a*, Chl *b*, total Chl, and Chl *a*/*b* ratio ($n = 4$). Pulse-amplitude modulated (PAM) fluorescence parameters include theoretical maximum yield of PSII (F_v/F_m), quantum yield of PSII (ΦII), quantum yield of ΦNPQ, and quantum yield of ΦNO ($n = 7$ for all PAM fluorescence parameters). D, The leaf ionome of each mutant line in comparison to the WT. The *y*-axis shows the modified *z*-score for a respective element in each line compared with WT ($n = 5–6$). Elements for which the modified *z*-score is greater than 1.0 are likely substantially different in concentration from WT in corresponding mutant. Rubidium (Rb^+) uptake over time as a proxy for Potassium (K^+) uptake in (E) shoots and (F) roots of hydroponically grown

(Continued)

and severe salt sensitivity (Wu et al., 1996; Zhu et al., 1998; Shi et al., 2002). Publicly available data from the ionomics database iHub confirm an average three-fold increase in Na accumulation in several untreated *sos1* null mutant alleles (Baxter et al., 2007).

Therefore, we generated two independent triple T-DNA insertion lines (Supplemental Figure S1 and Supplemental Table S1) *kea1-1kea2-1sos1-15* (ABRC stock: CS72656) and *kea1-2kea2-2sos1-16* (CS72657) and compared their respective phenotypic features to their parental lines (Figure 1 and Supplemental Figure S2). The introgression of both independent *sos1* loss-of-function insertions resulted in visibly reduced chlorosis in *kea1kea2sos1* plants without any additional NaCl input beyond what was already present in the growth substrate (Figure 1A and Supplemental Figure S2A). Concurrently, triple mutants had increased levels of Chl *a* and *b* compared with *kea1kea2* plants, but no alteration of Chl *a*/*b* ratio (Figure 1C). The additional loss of *SOS1* function in *kea1kea2* also partially relieved the suppression of photosynthesis as the theoretical maximum quantum efficiency of photosystem II (PSII) in the triple mutant increased compared with the double mutant (F_v/F_m; Figure 1, B and C and Supplemental Figure S2, B and C). The *kea1kea2sos1* line exhibited WT-level energy partitioning into photochemistry (ΦII) and regulated non-photochemical quenching (ΦNPQ), yet increased partitioning to nonregulated non-photochemical quenching (ΦNO; Figure 1C and Supplemental Figure S2C). In contrast, the *kea1kea2* double mutant exhibited decreased ΦII, increased ΦNPQ, and equivalent ΦNO compared with WT. These parameters indicate the *kea1kea2sos1* lines partition as much harvested photoenergy to electron transfer as the WT, at the cost of sustaining higher levels of photodamage. In contrast, *kea1kea2* partitions more energy to safe NPQ dissipation, thus minimizing photodamage, but at the cost of less energy routed toward photochemistry. Generally, the phenotypic trends for *kea1kea2sos1* mirror the published behavior for exogenous-salt treated *kea1kea2*, indicating that loss-of-function of *SOS1* is a genetic mechanism of phenotypic recovery for *kea1kea2*. A defect in *KEA1* and *KEA2* did not benefit the salt tolerance in triple mutants, that is *kea1kea2sos1* were similarly NaCl sensitive as *sos1* single mutant controls (Supplemental Figure S3).

Next, we investigated if the *kea1kea2sos1* recovery phenotype, that is reduced chlorosis and higher photosynthetic efficiency, corresponded with WT levels of various elements in leaf tissue (Figure 1D, Supplemental Figure S2D and Table 1, Supplemental Table S2). We used an established total X-ray fluorescence protocol (Höhner et al., 2016) to determine the ionome of rosettes from the WT, *kea1kea2*, *sos1*, and the triple mutant. To streamline the presentation of the ionomics data, we calculated a modified *z*-score akin to previous high-throughput ionomics experiments (Campos et al., 2021). *Z*-score is calculated as $\frac{|\mu_x - \mu_{wt}|}{s_x + s_{wt}}$, where μ_x and μ_{wt} represent the means of the mutant and the WT, and s_x and s_{wt} represent the standard deviations. A mutant allele *z*-score greater than 1 indicates the mean concentration for a given element is substantially different from the WT. We also checked for statistically significant differences between all genotypes for each element (*P*-value < 0.05, Table 1 and Supplemental Table S2) based on Tukey's honest significant difference (HSD) test if data were normally distributed, or Pairwise Wilcoxon rank sum test if one or more genotypes did not exhibit normal distribution of values. Phosphorus (P) and rubidium (Rb) were significantly increased in both independent *kea1kea2* double mutant lines, replicating previous results (Höhner et al., 2019; DeTar et al., 2021). K levels were significantly increased in the *kea1-1kea2-1* with a similar trend recorded in the *kea1-2kea2-2* double mutant. Intriguingly, the concentrations of these elements dropped so much in *kea1kea2sos1* mutants that they did not differ from the WT, suggesting that the triple mutant ionome is mostly reset. This again reflects the effect recorded after exogenous Na^+ treatment of *kea1kea2* (DeTar et al., 2021) and indicates that the phenotypic rescue is linked to rebalancing the ionome.

We have previously shown that *kea1kea2* phenotypes coincide with K overaccumulation. We hypothesized that introgression of the *sos1* loss-of-function allele results in increased competition between K^+ and Na^+ for root-to-shoot translocation, thus preventing overaccumulation of K in the aerial tissues. To test this, we performed Rb^+ uptake assays as a proxy for K^+ import into plants. Arabidopsis plants of different genotypes were grown hydroponically in 50 mL conical tubes filled with ¼ Murashige–Skoog Medium for about 4 weeks total. At the beginning of the uptake experiment, the growth media was exchanged with 1 mM rubidium (dissolved in 2.5 mM MES, pH 5.8 with KOH) for 24 h in total, with sampling of shoot (Figure 1E) and root (Figure 1F) tissue for Rb at regular intervals. We found significantly higher Rb transport into *kea1kea2* shoots compared with the WT after 8 and 24 h ($P < 0.05$, Tukey's HSD

Figure 1 (Continued)
plants (±SD). Asterisks denote points which are significantly different from the WT at a given timepoint ($n = 3$, $P < 0.05$ from Tukey's HSD or pairwise Wilcoxon rank sum test). G, Representative RNA probing of plastid rRNAs from aforementioned genotypes. Fragment sizes are indicated on the right-hand side of each blot in kilonucleotides (knt). Map of probe binding positions and expected fragments shown in Supplemental Figure S4A. Asterisks indicate fragments with altered abundance in the *kea1kea2* mutant ($n = 2$; biorep shown in Supplemental Figure S4B). H, Representative immunoblot of chloroplast proteins on leaf extracts from WT (three concentrations), *sos1-15*, *kea1-1kea2-1*, and *kea1-1kea2-1sos1-15* mutants ($n = 2$; accompanying Coomassie-stained gel shown in Supplemental Figure S4C, bioreplicate shown in Supplemental Figure S4D). I, The expression of the GOLDEN-LIKE 1 (*GLK1*) transcription factor based on RT-qPCR (±SD, $n = 3$). Asterisks denote points which are significantly different from the WT (*P*-value < 0.05 based on Tukey's HSD test).

Table 1 Leaf elements of WT and mutant alleles

Element	WT		*sos1-15*			*kea1-1kea2-1*			*kea1-1kea2-1sos1-15*		
	Conc. ($\mu g*mg^{-1}$ DW)	Std. Dev	Conc. ($\mu g*mg^{-1}$ DW)	Std. Dev	Mod. Z-score	Conc. ($\mu g*mg^{-1}$ DW)	Std. Dev	Mod. Z-score	Conc. ($\mu g*mg^{-1}$ DW)	Std. Dev	Mod. Z-score
Phosphorus	9.89	2.03	10.4	2.27	0.12	**15.9**※	**1.97**	**1.50**	12.0	1.16	0.77
Sulfur	8.57	3.85	8.66	4.00	0.01	9.47	2.23	0.15	8.77	2.45	0.00
Chlorine	0.640	0.660	0.482	0.270	0.17	0.361	0.141	0.35	0.285	0.127	0.59
Potassium	40.0	3.85	39.9	4.04	0.01	**50.8**※	**5.44**	**1.17**	42.9	4.80	0.13
Calcium	44.2	5.93	46.6	11.62	0.14	48.1	6.76	0.31	50.3	12.34	0.14
Manganese	0.055	0.020	0.061	0.029	0.12	0.045	0.021	0.25	0.058	0.024	0.46
Iron	0.061	0.022	0.068	0.021	0.17	0.075	0.022	0.31	0.096	0.035	0.31
Nickel	0.001	0.000	0.001	0.000	0.26	0.002	0.001	0.30	0.004	0.004	0.09
Copper	0.006	0.001	0.007	0.000	0.68	0.007	0.001	0.80	0.007	0.000	0.46
Zinc	0.160	0.064	0.121	0.014	0.50	0.113	0.008	0.64	0.104	0.008	0.83
Rubidium	0.010	0.001	0.010	0.001	0.12	**0.015**※	**0.002**	**1.40**	0.012	0.003	0.48
Strontium	0.048	0.012	0.051	0.013	0.10	0.051	0.009	0.13	0.053	0.014	0.02

Bold values with ※ indicate means statistically different from all other genotypes for that element ($n = 3$ for Cu and Zn; $n = 5–6$ for all other elements, P-value < 0.05 with Tukey's honest significance test or pairwise Wilcoxon rank sum test if one or more genotype did not exhibit normal distribution of values).

or pairwise Wilcoxon rank sum test). In the *kea1kea2sos1* triple mutant, shoot Rb was only significantly above WT at the 8 h data point, but not different from the WT after 24 h. All changes in root-level accumulation of Rb between genotypes were minor relative to the extreme accumulation of Rb in *kea1kea2* shoots. We interpret these data to suggest that loss of SOS1 in the *kea1kea2* background does not impair root-level uptake of K^+, but rather slows root-to-shoot translocation of K^+. Confirming other reports (Wu et al., 1996), we also found a slightly reduced root-to-shoot Rb^+ translocation in the *sos1* single mutant.

kea1kea2 plants have pronounced chloroplast rRNA maturation defects, which can be rescued by exogenous Na (DeTar et al., 2021). The lack of KEA1/2 transport activity may affect rRNA secondary structure and interactions with RNA processing factors. Thus, we evaluated how a *SOS1* loss-of-function influences rRNA maturation in *kea1kea2*. *kea1kea2sos1* triple mutants had lower levels of unprocessed *23S* rRNA precursors (Figure 1G, red asterisks, Supplemental Figure S4, A and B and Supplemental Table S3) compared with the *kea1kea2* mutant. The triple mutant also recovered WT levels of processed *4.5S* and *5S* rRNA (Figure 1G, red asterisks). As expected, the *sos1* single mutant did not show any plastid rRNA processing defects. Thus, rebalancing the ion homeostasis via *SOS1* loss-of-function also recovers rRNA processing in the *kea1kea2* background. Consequently, this should recover stromal protein synthesis and promote the expression of PhANGs. This was tested through immunoblotting of a subset of plastid-encoded proteins, including the large subunit of Rubisco (RbcL) and the D1 reaction center of PSII (PsbA). For nuclear-encoded plastid targeted proteins, we probed the LIGHT HARVESTING COMPLEX I (Lhcb1), the small subunit of Rubisco (RbcS), and TRANSLOCON AT THE INNER ENVELOPE MEMBRANE OF CHLOROPLASTS 110 (TIC110), a component of the protein import apparatus. We normalized loading of SDS gels to fresh weight rather than Chl or total protein to preclude any artificial biases in favor of the *kea1kea2* mutant, which has lower Chl content and reduced protein production (DeTar et al., 2021). In line with our previous study, the *kea1kea2* mutant exhibited decreased levels of plastid-encoded proteins RbcL and PsbA, which were partially recovered by introducing the *sos1* mutation (Figure 1H). The two PhANGs RbcS and Lhcb1 are known to be dynamically downregulated in response to loss of PGE. Indeed, both proteins were also downregulated in *kea1kea2*, yet recovered in *kea1kea2sos1*. TIC110 was slightly higher or unchanged in abundance in *kea1kea2* as observed before (DeTar et al., 2021). See Supplemental Figure S4C for Coomassie staining, that is protein loading corresponding to immunoblot in Figure 1H and Supplemental Figure S4D for an independent bioreplicate immunoblot. Collectively, our results suggest that both the nuclear-encoded and plastome-encoded portions of the plastid proteome are recovered by loss of *SOS1* in the *kea1kea2* mutant, as was observed with exogenous salt treatment (DeTar et al., 2021).

Finally, *KEA1/2* loss and subsequent disruption of PGE trigger GUN1-dependent RS to downregulate the expression of PhANGs (DeTar et al., 2021). This is mediated by suppression of the GOLDEN-LIKE 1 (*GLK1*) transcription factor (Waters et al., 2009; Martin et al., 2016). *GLK1* expression was quantified using RT-qPCR (Figure 1I). As previously observed, the expression of *GLK1* was significantly lower in *kea1kea2* compared with the WT. *GLK1* expression was unaffected in the *sos1* single mutant line and the *kea1kea2sos1* line compared with the WT ($P < 0.05$ based on Tukey's HSD test). These results explain the recovery of steady-state protein levels for the two PhANGs *LHCB1* and *RBCS*.

In summary, the additional loss-of-function of *SOS1* in the *kea1kea2* background induces a similar phenotypic recovery as observed when *kea1kea2* mutants are treated with exogenous Na. This shows that the exact mechanism of rebalancing K levels is less important to prevent the *kea1kea2* virescent phenotype, that is alleviate the defects

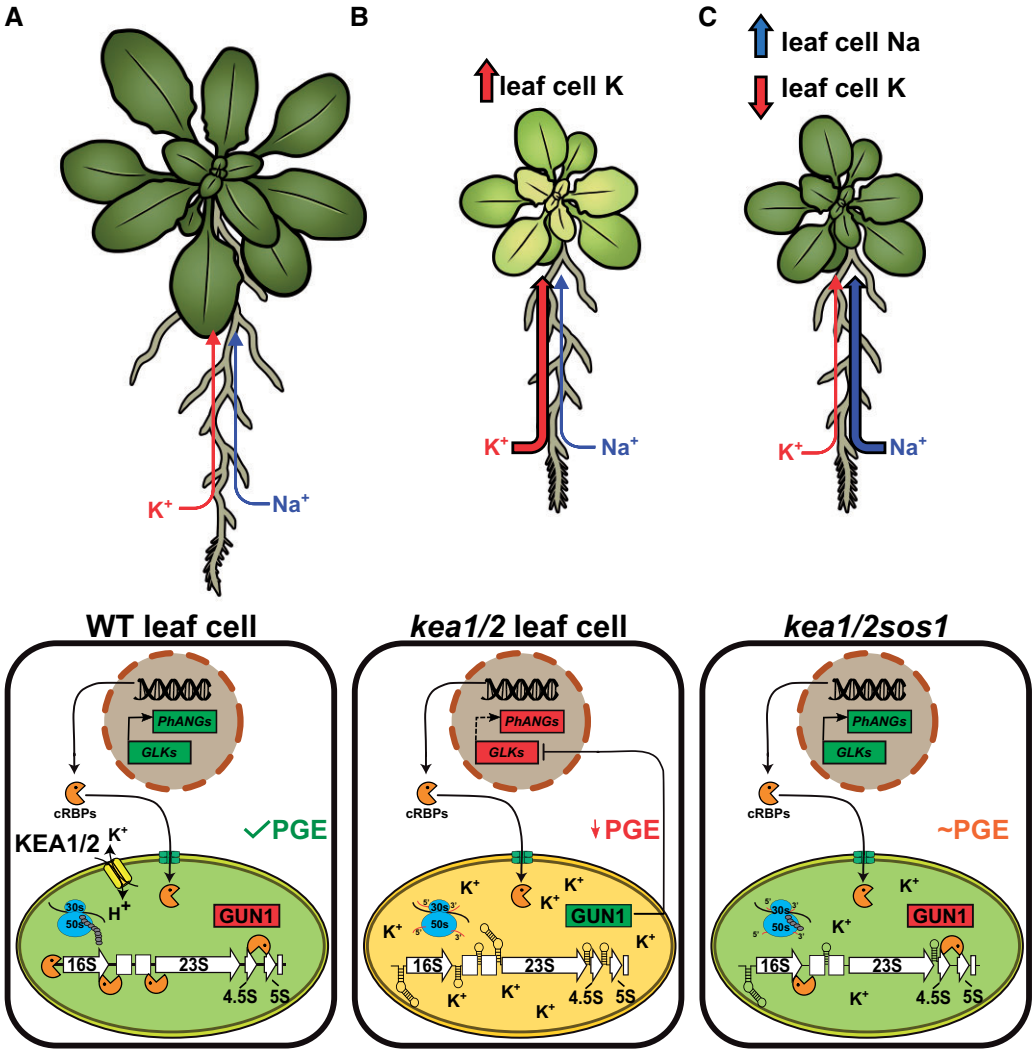

Figure 2 Model of *SOS1* loss-of-function-mediated recovery of *kea1kea2* phenotype. A, In WT leaf cells, potassium (K) equilibrium within the plant and the chloroplasts is maintained via K uptake and translocation. Optimal K level promotes plastid rRNA maturation and PGE. GLK1/PhANG expression in the nucleus progresses. B, In *kea1kea2*, K translocation into leaf tissue is increased compared with WT so that K accumulates in rosettes. Higher K disturbs proper stromal rRNA maturation and PGE, which activates GUN1 and RS resulting in *GLK1* and PhANG suppression. Hence, *kea1kea2* plants are small, chlorotic, and developmentally compromised. C, In *kea1kea2sos1* mutants, loss of *SOS1* leads to Na accumulation and less K translocation into rosettes, that is, K leaf levels are lower than in *kea1kea2*. This prevents perturbation of the chloroplast ionome and allows for proper rates of rRNA maturation and PGE. GUN1 and RS remain inactive which allows for the expression of *GLK1* and PhANGs. Consequentially, *kea1kea2sos1* plants are greener and more photosynthetically active. However, pleiotropic effects from the joint loss of *KEA1/2* and *SOS1* trigger ΦNO and prevent size recovery.

of chloroplast rRNA processing, PGE, and photosynthesis in the *kea1kea2* background. The Rb^+ uptake experiments indicate that root-level K^+ import is not per se higher in *kea1kea2*, but rather point to an increased root-to-shoot K^+ translocation in mutants compared with the WT (Figure 2, A and B). In contrast, *kea1kea2sos1* exhibits WT levels of root-to-shoot Rb/K translocation (Figure 2C). This provides evidence for the hypothesis that chloroplast K^+ transport may play a direct or indirect role in moderating overall plant K levels. While K is a key nutrient, our research has shown that plants can have too much of a good thing. Plants carefully maintain ion gradients not only to optimize membrane potentials and nutrition, but to minimize ion toxicity.

Supplemental data

The following materials are available in the online version of this article.

Supplemental Figure S1. Genotyping of *kea1kea2sos1* lines.

Supplemental Figure S2. Loss of *SOS1* results in phenotypic recovery of *kea1kea2* in independent lines.

Supplemental Figure S3. *kea1kea2sos1* alleles exhibit similar salt sensitivity as respective *sos1* lines.

Supplemental Figure S4. rRNA probe map and additional bioreplicates and loading controls for RNA and immunoblots.

Supplemental Table S1. Genotypes and primers used in this study.

Supplemental Table S2. Leaf elements of independent *kea1kea2* and *sos1* lines.

Supplemental Table S3. 80mer RNA probes used in this study.

Acknowledgments

We are grateful for technical undergrad assistance by WSU alumni: Eben Diederich, Simon Alsager, and Chase Baerlocher. Thanks to Drs. Benjamin Brandt and Serena Schwenkert for help with immunoblotting and Dr. Bettina Bölter (all LMU Munich) for critical reading of the manuscript. Special thanks to Susanne Mühlbauer from LMU for drawing the plants depicted in our model.

Funding

This work was supported by the National Science Foundation (NSF) Career Award IOS-1553506 to H.-H.K. and an NSF Graduate Research Fellowship Program to R.A.D. Furthermore, R.A.D. received funds from the NIH Biotechnology Training Program and the ARCS Foundation Fellowship. Elemental analysis was realized through an NSF MRI-1828266 award to H.-H.K. N.M. and J.M. were funded by DFG (SFB-TR 175, project A03). Lastly, H.-H.K. also received Deutsche Forschungsgemeinschaft (DFG) funds (SFB-TR 175, project B09).

Conflict of interest statement. None declared.

References

Aranda-Sicilia MN, Cagnac O, Chanroj S, Sze H, Rodríguez-Rosales MP, Venema K (2012) Arabidopsis KEA2, a homolog of bacterial KefC, encodes a K^+/H^+ antiporter with a chloroplast transit peptide. Biochim Biophys Acta **1818**: 2362–2371

Armbruster U, Carrillo LR, Venema K, Pavlovic L, Schmidtmann E, Kornfeld A, Jahns P, Berry JA, Kramer DM, Jonikas MC (2014) Ion antiport accelerates photosynthetic acclimation in fluctuating light environments. Nat Commun **5**: 5439

Baxter I, Ouzzani M, Orcun S, Kennedy B, Jandhyala SS, Salt DE (2007) Purdue ionomics information management system. An integrated functional genomics platform. Plant Physiol **143**: 600–611

Campos A, VanDijk W, Ramakrishna P, Giles T, Korte P, Douglas A, Smith P, Salt D (2021) 1,135 ionomes reveal the global pattern of leaf and seed mineral nutrient and trace element diversity in *Arabidopsis thaliana*. Plant J **106**: 536–554

DeTar RA, Barahimipour R, Manavski N, Schwenkert S, Höhner R, Bölter B, Inaba T, Meurer J, Zoschke R, Kunz H-H (2021) Loss of inner-envelope K^+/H^+ exchangers impairs plastid rRNA maturation and gene expression. Plant Cell **33**: 2479–2505

Höhner R, Galvis VC, Strand DD, Völkner C, Krämer M, Messer M, Dinc F, Sjuts I, Bölter B, Kramer DM, et al. (2019) Photosynthesis in Arabidopsis is unaffected by the function of the vacuolar K^+ channel TPK3. Plant Physiol **180**: 1322–1335

Höhner R, Tabatabaei S, Kunz HH, Fittschen U (2016) A rapid total reflection X-ray fluorescence protocol for micro analyses of ion profiles in *Arabidopsis thaliana*. Spectrochem Acta **125**: 159–167

Kunz H-H, Gierth M, Herdean A, Satoh-Cruz M, Kramer DM, Spetea C, Schroeder JI (2014) Plastidial transporters KEA1, -2, and -3 are essential for chloroplast osmoregulation, integrity, and pH regulation in Arabidopsis. Proc Natl Acad Sci USA **111**: 7480–7485

Martin G, Leivar P, Ludevid D, Tepperman JM, Quail PH, Monte E (2016) Phytochrome and retrograde signalling pathways converge to antagonistically regulate a light-induced transcriptional network. Nat Commun **7**: 10

Sánchez-McSweeney A, González-Gordo S, Aranda-Sicilia MN, Rodríguez-Rosales MP, Venema K, Palma JM, Corpas FJ (2021) Loss of function of the chloroplast membrane K^+/H^+ antiporters AtKEA1 and AtKEA2 alters the ROS and NO metabolism but promotes drought stress resilience. Plant Physiol Biochem **160**: 106–119

Shi H, Ishitani M, Kim C, Zhu JK (2000) The Arabidopsis thaliana salt tolerance gene SOS1 encodes a putative Na^+/H^+ antiporter. Proc Natl Acad Sci U S A **97**: 6896–6901

Shi H, Quintero FJ, Pardo JM, Zhu J-K (2002) The putative plasma membrane Na + /H + antiporter SOS1 controls long-distance Na^+ transport in plants. Plant Cell **14**: 465–477

Shin R, Adams E (2014) Transport, signaling, and homeostasis of potassium and sodium in plants. J Itegr Plant Biol **56**: 231–249

Wang C, Yamamoto H, Narumiya F, Munekage YN, Finazzi G, Szabo I, Shikanai T (2017) Fine-tuned regulation of the K^+/H^+ antiporter KEA3 is required to optimize photosynthesis during induction. Plant J **89**: 540–553

Waters MT, Wang P, Korkaric M, Capper RG, Saunders NJ, Langdale JA (2009) GLK transcription factors coordinate expression of the photosynthetic apparatus in Arabidopsis. Plant Cell **21**: 1109

Wu SJ, Ding L, Zhu JK (1996) SOS1, a genetic locus essential for salt tolerance and potassium acquisition. Plant Cell **8**: 617–627

Zhu JK, Liu J, Xiong L (1998) Genetic analysis of salt tolerance in Arabidopsis: evidence for a critical role of potassium nutrition. Plant Cell **10**: 1181–1191